Laser obscuration and infrared emission characteristics of red phosphorus and Mg-Al based smoke composition

Thang D. Pham[a], *Nhan* D. Phan[b], *Toan* T. Nguyen[c]

Le Quy Don Technical University, Faculty of Special Equipment

[a] Hanoi, Socialist Republic of Vietnam,
e-mail: thangpham@lqdtu.edu.vn,
ORCID iD: https://orcid.org/0000-0002-4377-8694

[b] e-mail: pdnhan912@yahoo.com,
ORCID iD: https://orcid.org/0000-0002-1947-2310

[c] e-mail: trungtoanktqs@mta.edu.vn, **corresponding author**,
ORCID iD: https://orcid.org/0000-0002-4753-9869

https://doi.org/10.5937/vojtehg74-58344

FIELD: pyrotechnic materials, chemical technologies
ARTICLE TYPE: original scientific paper

Abstract:

Introduction/purpose: The capability for laser attenuation and infrared (IR) radiation emission is one of the most essential characteristics determining the camouflage effectiveness of multispectral smoke screens on the battlefield. In this study, the effects of red phosphorus and Mg-Al content, the initial mass of the smoke composition, and the relative humidity on the obscuration characteristics of smoke cloud, including the degree of laser attenuation, the mass extinction coefficient, the Yield factor, and the Figure of Merit, were examined. Additionally, the IR emission properties of smoke screens based on RP/Mg-Al were also evaluated.

Methods: Laser radiation attenuation was evaluated by comparing the initial laser power to the power measured after passing through the smoke screen. A 1.064 μm, 11.0 mW continuous-wave laser was transmitted through the test chamber and measured with a power meter. The infrared properties of the smoke clouds were analyzed using an SR-5000N spectral radiometer within the 2.5 – 14.0 μm range.

Results: The results indicate that increasing the content of red phosphorus, sample masses, and relative humidity enhances the laser obscuration characteristics. Notably, for a 1 m^3 smoke chamber, the estimated optimal sample masses are 3.25 g and 2.30 g at 65% and 90% relative humidity, respectively. Furthermore, increasing Mg-Al content enhances IR emission in the β band (3-5 μm), while emission in the γ band (8-14 μm) decreased.

Conclusion: The laser obscuration characteristics of RP/Mg-Al-based smoke compositions can be effectively controlled by optimizing the RP/Mg-Al content and relative humidity levels. Moreover, the RP/Mg-Al-based

compositions demonstrate strong IR radiation characteristics, which are also influenced by the content of RP and Mg-Al. Future research should focus on evaluating the obscuration characteristics of RP/Mg-Al-based compositions in the near- and far-IR regions.

Keywords: multispectral smoke, obscuration performance, infrared radiation characteristics, red phosphorus, Mg-Al alloy.

Introduction

In modern warfare, laser technology is widely utilized in guidance systems, target acquisition, and rangefinding, while infrared (IR) technology enables surveillance, tracking, and thermal imaging (Lyubomir et al., 2021; Suliman & Kivrak, 2023). The rapid evolution of guided weapons and IR imaging devices has rendered traditional smoke screens, such as C_2Cl_6/C_6Cl_6 (HC smokes) and white phosphorus, ineffective in concealing combat vehicles on the battlefield (Harmata, 2018). Consequently, multispectral smoke screens are required to meet new demands, including effective attenuation of laser radiation and enhanced IR emission for jamming purposes (Koch, 2012). Red phosphorus (RP) smoke is effective at attenuating radiation in the laser (1.064 μm) and near-IR (0.7–1.4 μm) spectra, but it exhibits limited performance in the mid-IR (3–5 μm) and far-IR (8–14 μm) ranges. Incorporating high heat-generating fuels and fluorocarbon-based oxidizers into RP formulations enhances both laser attenuation and IR obscuration capabilities, providing effective countermeasures against laser-guided weapons and IR-based threat systems (Koch, 2008; Smit et al., 2009).

Previous studies have evaluated obscuration efficiency using parameters such as the degree of laser attenuation (A), the mass extinction coefficient (α_λ), the yield factor (Y_f), and the Figure of Merit (F_m), which are influenced by component ratios, initial mass (m_p), and relative humidity (RH). The role of H_3PO_4 droplets from RP oxidation in obscuring the 3-5 μm and 8-14 μm bands was highlighted (Suzuki, 2002). A 100% obscuration in the visible ranges and 76% in the 8-14 μm band was observed with the 80% RP and 20% KNO_3 mixture at 85% RH. Moreover, the α_λ values were 1.04 $m^2.g^{-1}$ (3-5 μm) and 0.85 $m^2.g^{-1}$ (8-14 μm) at 55% RH (Gautam et al., 2006). Effective attenuation of IR radiation at wavelengths of 0.82 μm, 3-5 μm, and 10.6 μm with high efficiency was achieved by the pyrotechnic charges composed of plasticized RP combined with epoxy resin. Specifically, the mixture of 55% RP, 12% Mg, 28% $NaNO_3$, and 5% resin achieved the α_λ value of 0.51 $m^2.g^{-1}$ (3-5 μm) and 0.36 $m^2.g^{-1}$ (10.6 μm) (Klusáček & Navrátil, 2004). Mg_4Al_3 alloy

powder was utilized as a high-energy fuel, achieving an α_λ of 1.44 $m^2 . g^{-1}$ at 1.064 μm (Cudziło & Trzcinski, 1999). Tests of 66 mm Buck MASKE RP smoke rounds on M1A1 Abrams and M88A2 Hercules vehicles were conducted, resulting in screening times of 60 s in the visible region and 30 s in IR bands (Smit et al., 2007).

Meanwhile, research on IR emission characteristics of RP-based smoke remains sparse. High IR emission in the 2-5 μm band was produced by a mixture of RP, Mg, and oxidizers (Teflon/KNO_3), with a 1.5 m thick smoke layer at 2 $g.m^{-3}$ (Cudziło, 2001). The addition of 20% RP to an Mg/PTFE/Viton mixture was observed to enhance the radiating area and intensity with minimal impact on radiation itself (Li et al., 2017). A composition of 59% RP, 21% Zr, 15% KNO_3, and 5% polyacrylate binder was found to exhibit greater spectral energy in the (8-14 μm) band than the (3-5 μm) band. The γ/β band ratio and spectral energy suggest that the combustion flame of the pyrolant cannot be characterized as a graybody (Koch, 2022). It is evident that studies on the obscuration and IR emission characteristics of RP-based smoke have shown notable results. However, the available research on the RP and Mg-Al-based multispectral smoke formulations remains limited.

This work investigates the obscuration behaviors and IR emission properties of RP/Mg-Al-based smoke screens. The effects of various factors, such as RP and Mg-Al content, sample mass, and relative humidity on the obscuration characteristics, including the degree of laser attenuation, the mass extinction coefficient, the Yield factor, and the Figure of Merit were examined under 1.064 μm laser radiation. Moreover, IR emission properties, such as spectral radiance and emission distribution, were measured with a spectroradiometer that covered the wavelength range of 2.5-14 μm.

Materials and methods

Materials

The raw materials employed in this study comprised Mg-Al alloy powder (50:50 wt.%), polytetrafluoroethylene (PTFE) powder, red phosphorus (RP) powder, and sodium nitrate ($NaNO_3$) powder, all sourced from Shanghai Macklin Biochemical Co., Ltd. The commercial grade Viton A rubber (vinylidene fluoride-hexafluoropropene copolymer, 66 wt.% fluorine content) was obtained from DuPont Company (Wilmington, DE, USA). Analytical grade acetone (CH_3COCH_3) was purchased from Xilong Co., Ltd. Technical specifications of the investigated materials are summarized in Table 1.

Table 1 - Several technical parameters of the materials

Materials	Molecular formula	Purity, %	Mean size, μm
Red phosphorus	P	≥ 99	40
Magnesium- Aluminum Alloy	Mg-Al	≥ 98	74
Teflon (PTFE)	$(C_2F_4)_n$	≥ 99	20
Sodium nitrate	$NaNO_3$	≥ 98	60
Manganese dioxide	MnO_2	≥ 98	10
Viton A	$C_{10}H_7F_{13}$	≥ 99	-
Acetone	C_3H_6O	≥ 99.5	-

Experiment and methods

Sample preparation

The mixture containing Mg-Al alloy, PTFE, $NaNO_3$, and MnO_2 powders (MAT mixture) was mixed through a 0.5 mm silk sieve. A binder solution was prepared by dissolving Viton A rubber in acetone at a 1:15 w/v ratio. After adding the MAT mixture and RP to the binder solution, the mixture was stirred at 600 rpm for 30 minutes to prepare the MATV-RP mixture. The obtained MATV-RP mixture was passed through a 1.25 mm mesh and was air-dried for 30 minutes. Final drying was carried out under at 55 °C for 5 hours. The preparation process and the components of MATV-RP mixture are expressed in Figure 1 and Table 2.

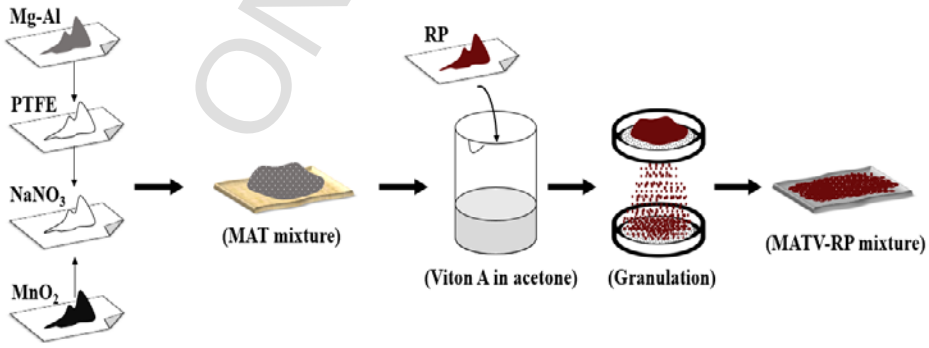

Figure 1 - The preparation process diagram of MATV-RP mixture

Table 2 - The components of MATV-RP mixture

Samples	Content (%)					
	RP	Mg-Al	PTFE	$NaNO_3$	MnO_2	Viton A
M1	40	35	10	6.5	0.5	8
M2	45	30	10	6.5	0.5	8
M3	50	25	10	6.5	0.5	8
M4	55	20	10	6.5	0.5	8
M5	60	15	10	6.5	0.5	8
M6	65	10	10	6.5	0.5	8

Experimental techniques

The experimental setup for measuring the obscuration characteristics of the smoke screen under 1.064 μm laser radiation is illustrated in Figure 2.

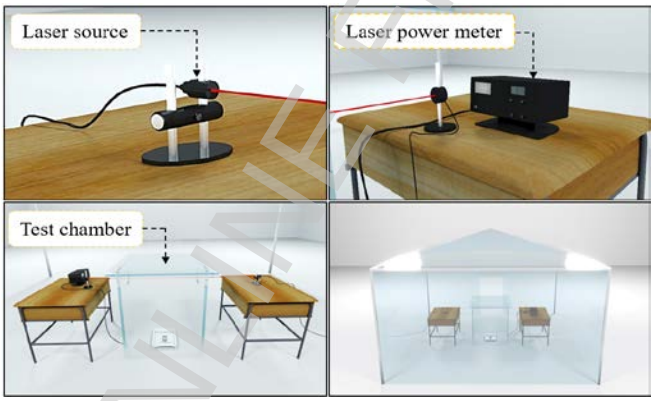

Figure 2 - Experimental setup for measuring the obscuration characteristics

The degree of laser radiation attenuation was determined by comparing the initial laser power (without obscuring) with the laser power measured after passing through the screening smoke. A 1.064 μm continuous-wave laser source with an output power of 11.0 mW was directed through the cubical test chamber and measured by a laser power meter. The total path length through the screening smoke was 600 mm. The transmittance T (i.e., the degree of transmission) was determined using the formula (Cudziło & Papliński, 1999):

$$T = \frac{I_{min}}{I_0} \tag{1}$$

where, I_0 and I_{min} are the initial laser intensity without smoke and the minimum laser intensity after passing through the screening smoke, respectively.

The degree of laser attenuation (A) can be calculated using the following formula (Koch, 2012):

$$A(\%) = (1 - T).100 \quad (2)$$

The mass extinction coefficient α_λ ($m^2.g^{-1}$) is derived from the Lambert-Beer law through the following expression (Kiteto & Mecha, 2024; Koch, 2012):

$$\alpha_\lambda = -\frac{\ln T}{C.L} \quad (3)$$

where C is the smoke concentration ($g.m^{-3}$); L is the thickness of the smoke screen (m).

The Yield factor Y_f of the smoke composition typically represents the ratio of the mass of the aerosol m_s to the initial mass of the smoke composition m_p. Essentially, it measures how efficiently the material contributes to producing the desired smoke effect. Mathematically, it could be expressed as (Koch, 2012):

$$Y_f = \frac{m_s}{m_p} \quad (4)$$

To comprehensively assess the camouflage capability of a smoke composition, the concept of the Figure of Merit (F_m) is commonly used, which is the product of the Yield factor and the mass extinction coefficient (Koch, 2012):

$$F_m = \alpha_\lambda.Y_f \quad (5)$$

The IR radiation characteristics of smoke clouds were measured by the spectral radiometer (SR-5000N, CI systems) with a working wavelength from 2.5-14.0 μm (Figure 3). 15 grams of the sample were burned using an electric primer in a cubic test chamber with a volume of 0.216 m^3.

The lenses of the radiometer were positioned facing the smoke cloud through a source window on the wall of the test chamber, and the distance between the lenses and the source window was approximately 5.0 m. The emission intensity was scanned every second within the 2.5-14.0 μm wavelength range and repeated. The IR emission intensity and radiance were determined using the built-in software.

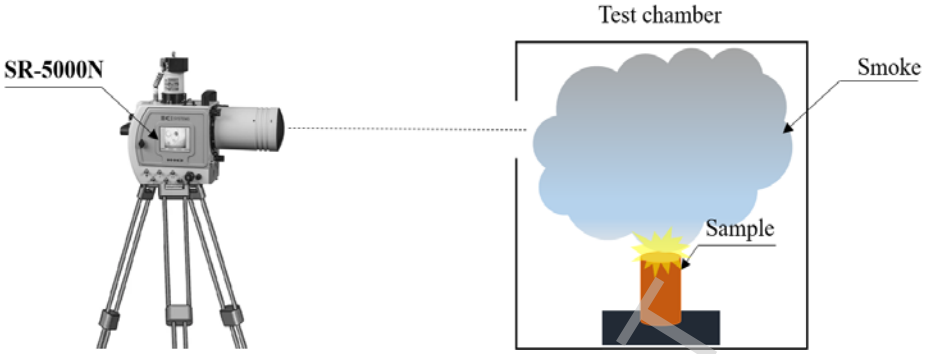

Figure 3 - Experimental setup for measuring the IR emission characteristics

The radiance distribution function for the wavelength range from λ_1 to λ_2 describes the radiance of an emissive surface within that specific range, represented as $L(\lambda_1-\lambda_2)$ ($W.sr^{-1}.cm^{-2}$) (Arecchi et al., 2007).

$$L_{(\lambda_1-\lambda_2)} = \int_{\lambda_1}^{\lambda_2} L_\lambda(\lambda).d\lambda \quad (6)$$

Results and discussion

Effect of RP content on the obscuration characteristics

The obscuration characteristics of M1-M6 samples at different relative humidity levels are presented in Table 3. It should be noted that the initial mass of the smoke composition m_p was fixed at 0.5 grams and the RP content was increased from 40-65%, as detailed in Table 2. The smoke concentration *C* was theoretically computed based on the free energy minimization method (Belov, 1998).

The results indicate that increasing RP content enhances the smoke concentration C and Yield factor Yf, resulting in higher mass extinction coefficient αλ and Figure of Merit Fm, while the transmittance T decreased significantly. When the mp is fixed, a higher RP content increases the actual mass of RP, resulting in enhanced smoke production and elevated concentrations of combustion products (P2, P4) (Toan et al., 2022). Notably, the obtained Yield factors (Yf = 1.59-2.22) are higher than those reported for Ti/poly-carbon monofluoride and Mg/poly-carbon monofluoride (Yf = 1.0-1.2), as well as RP/Mg/Teflon-based compositions (Yf = 0.8) (Cudziło & Trzcinski, 1999), reflecting the superior obscuration

capabilities of RP/Mg-Al-based smoke for enhanced protection against laser irradiation.

Table 3 - Effect of RP content on obscuration characteristics at 65% and 90% RH

Samples	Mass of RP (gram)	C, (g.m-3)	Yf	65% RH			90% RH		
				T, (%)	αλ, (m2.g-1)	Fm, (m2.g-1)	T, (%)	αλ, (m2.g-1)	Fm, (m2.g-1)
M1	0.20	3.68	1.59	22	0.69	1.09	12	0.96	1.53
M2	0.23	3.96	1.71	18	0.72	1.23	08	1.06	1.82
M3	0.25	4.26	1.84	15	0.74	1.37	06	1.10	2.03
M4	0.28	4.58	1.98	07	0.97	1.91	05	1.11	2.16
M5	0.30	4.87	2.10	06	0.98	2.03	04	1.13	2.32
M6	0.38	5.13	2.22	03	1.14	2.52	02	1.27	2.82

Furthermore, higher relative humidity enhances water absorption by H_3PO_4 droplets, leading to larger smoke particles that contribute to increased the mass extinction coefficient α_λ and Figure of Merit F_m (Milham et al., 1982). The obtained α_λ values are higher than those of RP/KNO_3 mixture in the spectral ranges of (3-5 µm) and (8-14 µm) (Gautam et al., 2006). Moreover, the F_m values obtained at 65% RH are comparable to those reported for mixtures containing RP, Mg_4Al_3, $Ba(NO_3)_2$, and Viton A (Toan et al., 2022). Overall, the combination of higher RP content and elevated RH substantially enhances both the mass extinction coefficient and Figure of Merit, thereby optimizing the camouflage performance of the smoke screen.

The degree of laser radiation attenuation A at different RP content and RH is presented in Figure 4 and Table 4.

The maximum A_{max} and average A_{avg} attenuation levels, as well as the screening time for maintaining over 85% laser radiation attenuation ($t_{A > 85\%}$), increased with higher RP content and relative humidity. Additionally, the differences in attenuation (ΔA_{max} and ΔA_{avg}) decreased at higher RP contents, suggesting the need to consider both parameters for practical applications. Notably, at RP contents ≥ 55% and 90% RH, $t_{A > 85\%}$ exceeded 200s, highlighting optimal and sustained screening performance (Table 4).

Based on these experimental results, the optimal RP content for achieving effective camouflage depends on the humidity level. Specifically, at 65% RH (Figure 4a), an RP content of 60–65% is recommended to maximize attenuation and ensure sustained performance, compensating

for lower moisture conditions. In contrast, at 90% RH (Figure 4b), an RP content of 55–60% is sufficient to provide robust and prolonged attenuation, optimizing material efficiency under elevated humidity.

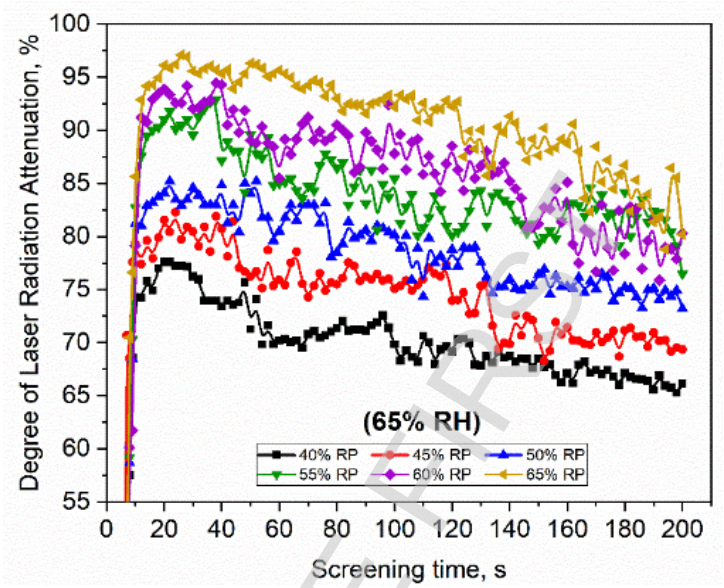

(a)

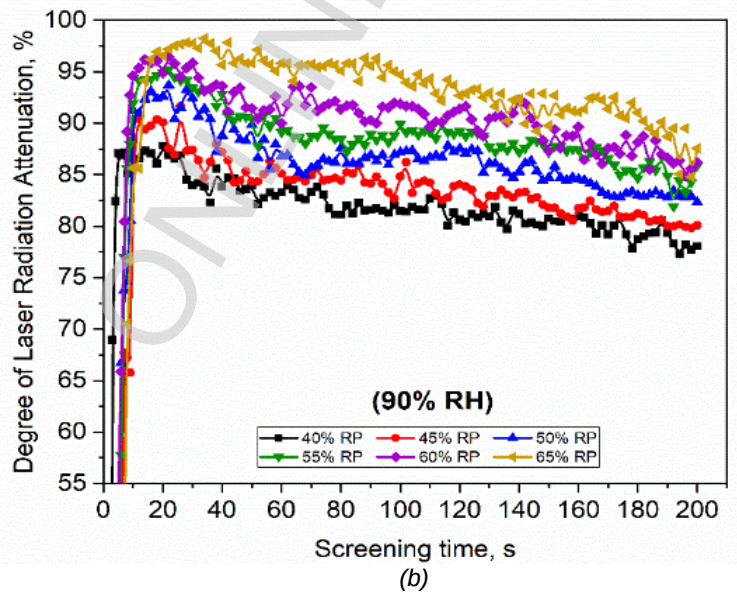

(b)

Figure 4 - The degree of laser radiation attenuation at 65% RH (a) and 90% RH (b)

Table 4 - The degree of laser radiation attenuation as a function of RP content and RH

Samples	RP, %	RH, %	Amax, %	ΔAmax, %	Aavg, %	ΔAavg, %	tA > 85%, s
M1	40	65	77.60	10.23	69.99	11.64	0
		90	87.84		81.63		30
M2	45	65	82.29	9.35	74.48	9.15	0
		90	91.64		83.64		30
M3	50	65	85.18	8.52	78.74	7.60	0
		90	93.70		86.34		60
M4	55	65	92.92	2.32	84.22	4.40	90
		90	95.24		88.61		>200
M5	60	65	94.44	2.01	86.30	4.21	150
		90	96.45		90.51		>200
M6	65	65	97.11	1.13	90.89	2.57	>200
		90	98.24		93.46		>200

Effect of sample mass on the obscuration characteristics

The effect of sample mass m_p on the degree of laser radiation attenuation of the M5 sample under different relative humidity is presented in Figure 5 and Table 5.

It can be seen that the combination of increased sample mass m_p and elevated RH is critical for sustaining effective laser radiation attenuation. When $m_p \leq 0.3$ g, RH exhibits a significant impact on the degree of laser radiation attenuation, as evidenced by the changes in ΔA_{max} and ΔA_{avg}. As a result, the smoke screen is unstable and fails to maintain coverage above 85%. However, the influence of RH on the degree of laser radiation attenuation becomes negligible when $m_p \geq 0.5$ g. The samples exhibit high $t_{A > 85\%}$ values (> 200s), particularly at 90% RH (Figure 5b and Table 5). A notable observation is that once the optimal mass threshold is reached (m_p = 0.7 g at 65% RH and m_p = 0.5 g at 90% RH), further increases in m_p result in negligible improvements in laser attenuation. Based on the experimental results, the optimal m_p for a 1 m^3 smoke chamber at different RH levels can be estimated as follows: m_p = 3.25 g at 65% RH and m_p = 2.30 g at 90% RH.

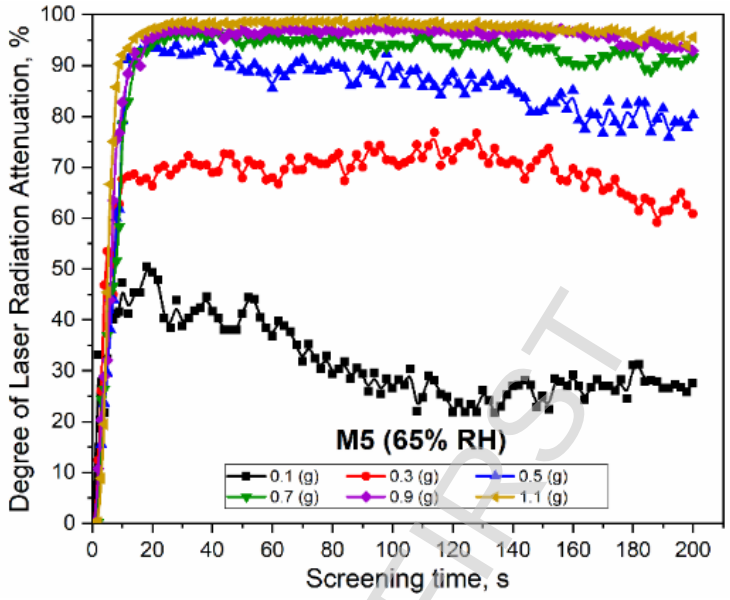

(a)

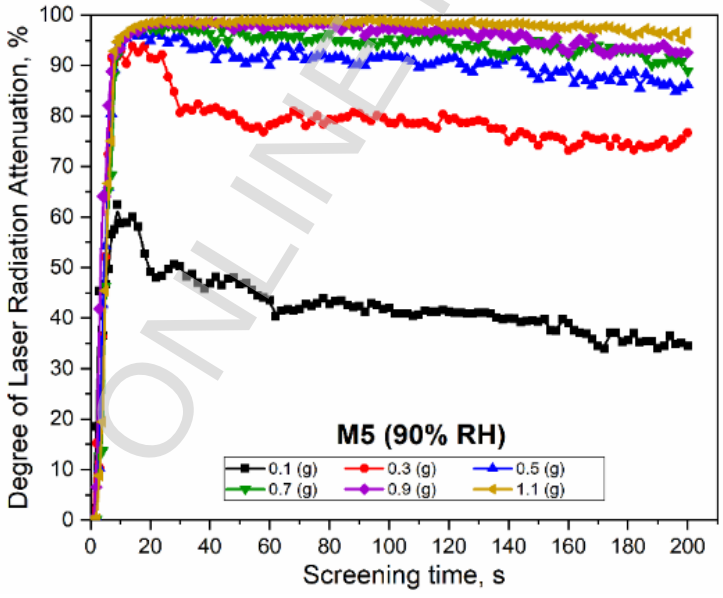

(b)

Figure 5 - Effect of sample mass on the degree of laser radiation attenuation of M5 sample at 65 %RH (a) and 90% RH (b)

Table 5 - The degree of laser radiation attenuation as a function of mp and RH

m_p, g	RH, %	A_{max}, %	ΔA_{max}, %	A_{avg}, %	ΔA_{avg}, %	$t_{A>85\%}$, s
0.1	65	50.41	12.00	31.67	10.53	0
	90	62.41		42.20		0
0.3	65	76.87	16.98	69.48	9.67	0
	90	93.86		79.16		30
0.5	65	94.44	2.01	86.47	4.31	150
	90	96.45		90.78		>200
0.7	65	96.49	1.37	93.35	1.16	>200
	90	97.86		94.51		>200
0.9	65	97.58	1.05	95.90	0.39	>200
	90	98.63		96.28		>200
1.1	65	98.92	0.22	97.52	0.58	>200
	90	99.14		98.11		>200

Infrared radiation properties

The average IR radiance values of the RP/Mg-Al-based smoke composition were measured using the SR-5000N Radiometer, with the $L_{(\lambda 1-\lambda 2)}$ values calculated according to Eq. (6), and the results are presented in Table 6 and Figure. 6.

The experimental results indicate that all samples (M1-M6) emit IR radiation in both *β* band (3-5 μm) and *γ* band (8-14 μm). However, the intensity distribution of IR radiation shows a clear inverse relationship between the two wavelength bands, which is fundamentally influenced by the compositional characteristics of the sample.

It can be noted that increasing the Mg-Al content leads to an increase in IR radiation in the *β* band, while the IR radiation in the *γ* band decreases. Table 6 shows that M1 has the highest IR radiation in the *β* band at 8.266 (10^{-2} .W.sr^{-1}.cm^{-2}), while M6 has the lowest at 2.195 (10^{-2}.W.sr^{-1}.cm^{-2}). Conversely, in the *γ* band, M6 achieves the highest radiation emission at 4.435 (10^{-2}.W.sr^{-1}.cm^{-2}), while M1 records the lowest at 1.270 (10^{-2}.W.sr^{-1}.cm^{-2}). This observation can be explained by the fact that M1 has higher Mg-Al content, resulting in stronger IR radiation in the *β* band, while M6, with higher RP content, shows higher *γ* band radiation (Toan et al., 2022). This variation indicates that chemical constituents affect IR emission.

Table 6 - The radiance distribution of MATV-RP samples

Samples	RP, %	Mg-Al, %	$L_{(\lambda 1-\lambda 2)}$, ($10^{-2}$.W.sr^{-1}.cm^{-2})		
			β band (3-5 μm)	*γ* band (8-14 μm)	*γ/β* band ratio
M1	40	35	8.266	1.270	0.154
M2	45	30	6.987	1.528	0.219
M3	50	25	5.171	2.557	0.494
M4	55	20	4.394	3.434	0.782
M5	60	15	2.879	3.717	1.291
M6	65	10	2.195	4.435	2.021

The γ/β ratio increases markedly from 0.154 for M1 to 2.201 for M6 (Figure 6a). This highlights that compositional changes impact both the intensity of radiation and its distribution (Figure 6b) between the two spectral regions, suggesting that optimizing the Mg-Al to RP ratio could yield smoke compositions with desired IR properties for specific applications. Notably, the γ/β band ratio observed in the M5 sample (γ/β = 1.291) aligns closely with the value (γ/β = 1.270) previously reported for a composition consisting of 59% RP, 21% Zr, 15% KNO_3, and 5% polyacrylate binder (Koch, 2022).

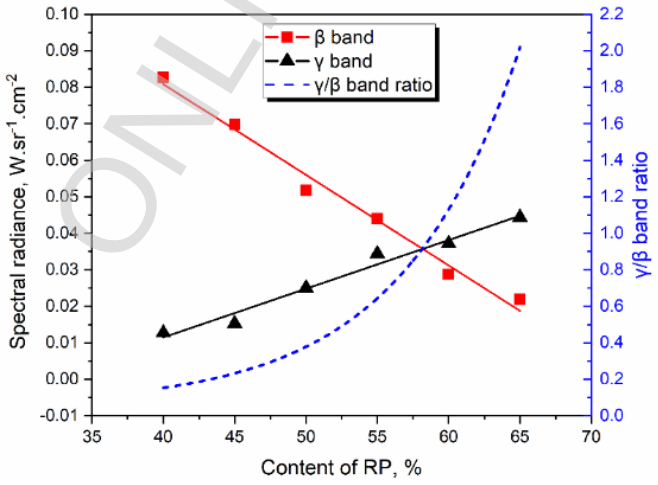

(a)

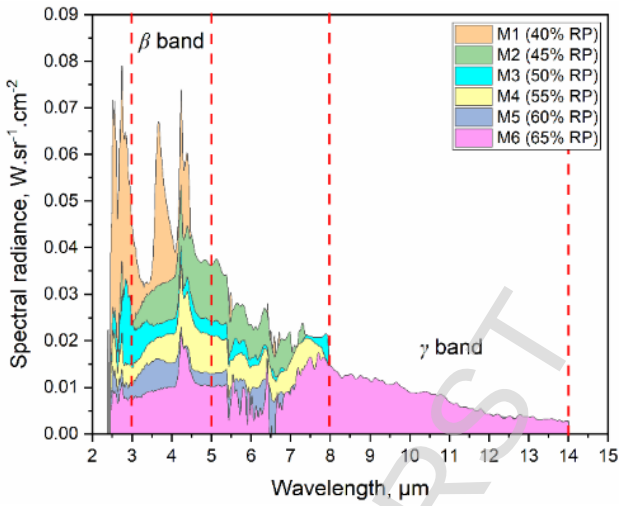

(b)

Figure 6 - Effect of RP and Mg-Al content on the intensity of radiation (a) and its distribution (b) in the β and γ band

Conclusions

The laser obscuration characteristics of RP/Mg-Al-based smoke compositions can be effectively controlled by optimizing the content of RP/Mg-Al and RH levels. Increasing RP content enhances the mass extinction coefficient α_λ, the Yield factor Y_f, and the Figure of Merit F_m, while reducing the transmittance T. At high humidity (90% RH), the degree of laser attenuation significantly improves with the screening time for maintaining over 85% attenuation exceeding 200 seconds, superior to low humidity conditions (65% RH). The initial sample mass m_p greatly influences laser radiation attenuation. For a 1 m^3 smoke chamber, the estimated optimal sample masses are 3.25 g and 2.30 g at 65% and 90% RH, respectively.

In addition to providing effective laser attenuation, the RP/Mg-Al-based compositions demonstrate strong IR radiation characteristics, which are also influenced by the content of RP and Mg-Al. All samples emit IR radiation in both the β (3-5 μm) and γ (8-14 μm) bands. The γ/β ratio exhibits an increase from M1 to M6, demonstrating the capacity to optimize IR radiation through the RP/Mg-Al ratio.

Future research should focus on evaluating the obscuration characteristics of the RP/Mg-Al-based composition in the near and far-IR regions.

References

Arecchi, A. V., Koshel, R. J. & Messadi, T. 2007. *Field guide to illumination*, SPIE Bellingham, WA, USA. Available at: https://doi.org/10.1117/3.764682

Belov, G. V. 1998. Thermodynamic analysis of combustion products at high temperature and pressure. *Propellants, explosives, pyrotechnics,* 23**,** pp.86-89. Available at: https://doi.org/https://doi.org/10.1002/(SICI)1521-4087(199804)23:2<86::AID-PREP86>3.0.CO;2-2

Cudziło, S. 2001. Studies of IR-Screening Smoke Clouds. *Propellants, Explosives, Pyrotechnics,* 26**,** pp.12-16. Available at: https://doi.org/10.1002/1521-4087(200101)26:1

Cudziło, S. & Papliński, A. 1999. An Influence of the Chemical Structure of Smoke-Generating Mixtures on Laser Radiation Attenuation at 1.06-μm and 10.6-μm Wavelengths. *Propellants, Explosives, Pyrotechnics,* 24**,** pp.242-245. Available at: https://doi.org/10.1002/(SICI)1521-4087(199908)24:4

Cudziło, S. & Trzcinski, W. 1999. Comparison investigations of camouflage capability of different pyrotechnic smoke compositions in IR region. 7th International Seminar EURPOPYRO'99, pp 7-11.

Gautam, G., Joshi, A., Joshi, S., Arya, P. & Somayajulu, M. 2006. Radiometric screening of red phosphorus smoke for its obscuration characteristics. *Defence Science Journal,* 56**,** pp.377-381. Available at: https://doi.org/10.14429/dsj.56.1903

Harmata, W. 2018. Smoke as a component of military camouflage systems. *Bulletin of the Military University of Technology,* 67**,** pp.83-113. Available at: https://doi.org/10.5604/01.3001.0012.6600

Kiteto, M. & Mecha, C. 2024. Insight into the Bouguer-Beer-Lambert Law: A review. *Sustainable Chemical Engineering***,** pp.567-587. Available at: https://doi.org/10.37256/sce.5220245325

Klusáček, L. & Navrátil, P. 2004. The Use and Application of Red-Phosphorous Pyrotechnic Composition for camouflage in the infrared region of radiation. *Propellants, Explosives, Pyrotechnics,* 22**,** pp.74-77. Available at: https://doi.org/10.1002/prep.19970220205

Koch, E.-C. 2008. Special Materials in Pyrotechnics: V. Military Applications of Phosphorus and its Compounds. *Propellants, Explosives, Pyrotechnics,* 33**,** pp.165-176. Available at: https://doi.org/10.1002/prep.200700212

Koch, E.-C. 2012. Obscurants. *Metal-Fluorocarbon Based Energetic Materials.* pp.197-199. Available at: https://doi.org/10.1002/9783527644186.ch11

Koch, E.-C. 2022. Radiative Properties of a Red Phosphorus Based Combustion Flame. *Central European Journal of Energetic Materials,* 19**,** pp.5-17. Available at: https://doi.org/10.22211/cejem/147623

Li, J., Chen, X., Wang, Y., Shi, Y. & Shang, J. 2017. Burning and radiance properties of red phosphorus in Magnesium/PTFE/Viton (MTV)-based compositions. *Infrared Physics & Technology,* 85**,** pp.109-113. Available at: https://doi.org/10.1016/j.infrared.2017.06.002

Lyubomir, L., Edmunds, T. & Risham Singh, G. 2021. Applications of laser technology in the army. *Journal of Defense Management,* 11**,** pp.1-8. Available at: https://doi.org/10.35248/2167-0374.21.11.210

Milham, M. E., Anderson, D. & Frickel, R. H. 1982. Infrared optical properties of phosphorus-derived smoke. *Applied Optics,* 21**,** pp.2501-2507. Available at: https://doi.org/10.1364/AO.21.002501

Smit, K., Lee, A. & Burridge, M. Smoke countermeasure testing for the M1A1 Abrams. Proc. Land Warfare Conference, Adelaide, South Australia, 2007. Available at: https://www.researchgate.net/publication/340684654

Smit, K., Lee, A. & Burridge, M. Smoke Countermeasures for Army in the Visual and Infrared. 36th International Pyrotechnics Seminar, 2009 Rotterdam, The Netherlands. Available at: : https://www.researchgate.net/publication/340684572

Suliman, H. M. & Kivrak, S. 2023. Anti-Tank Guided Missile System Design Based on an Object Detection Model and a Camera. *International Journal of Computational Intelligence Systems,* 16, pp.20. Available at: https://doi.org/10.1007/s44196-023-00198-6

Suzuki, Y. M., K. & Suzuki, Y. 2002. IR-Screening properties of red phosphorus smoke. *Kayaku Gakkaishi,* 63**,** pp.185-190. Available at: https://www.jes.or.jp/mag_eng/stem/Vol.63/documents/Vol.63,No.4,p.185-190

Toan, N. T., Tinh, N. V. & Sang, D. Q. 2022. Obscurant and Radiation Characteristics of Infrared Screening Smoke Composition Based on Red Phosphorus. *Defence Science Journal,* 72**,** pp.353-358. Available at: https://doi.org/10.14429/dsj.72.17676

Karakteristike zaklanjanja lasera i emisije infracrvenog zračenja dimne smeše na bazi crvenog fosfora i legure Mg-Al

Thang D. Pham, *Nhan* D. Phan, *Toan* T. Nguyen, **autor za prepisku**
Le Quy Don Technical University, Faculty of Special Equipment,
Hanoi, Socialist Republic of Vietnam

OBLAST: pirotehnički materijali, hemijske tehnologije
KATEGORIJA (TIP) ČLANKA: originalni naučni rad

Sažetak:

Uvod/cilj: Sposobnost prigušivanja laserskog zračenja i emisije infracrvenog zračenja predstavlja jednu od ključnih karakteristika koje utiču na kamuflažnu efikasnost multispektralnih dimnih zavesa na bojnom polju. Ovaj rad ispituje uticaje sadržaja crvenog fosfora i legure Mg-Al, početne mase dimnog sastava i relativne vlažnosti vazduha na karakteristike zaklanjanja dimnog oblaka, uključujući stepen prigušenja lasera, masu koeficijenta ekstinkcije, faktor efikasnosti generisanja aerosola i faktor kvaliteta. Takođe, u radu su analizirane i osobine infracrvenog zračenja dimnih zavesa na bazi crvenog fosfora i legura Mg-Al (RP/Mg-Al).

Metode: Prigušenje laserskog zračenja određivano je upoređivanjem početne snage lasera sa snagom izmerenom nakon prolaska kroz dimnu zavesu. Kroz ispitnu komoru emitovan je kontinuirani laser talasne dužine 1,064 μm i izlazne snage 11,0 mW, a snaga je merena pomoću laserskog merača snage. Infracrvene osobine dimnih oblaka analizirane su spektralnim radiometrom SR-5000N u opsegu talasnih dužina od 2,5 do 14,0 μm.

Rezultati: Rezultati pokazuju da povećanje sadržaja crvenog fosfora, mase uzoraka i relativne vlažnosti vazduha poboljšava karakteristike laserskog zaklanjanja. Za komoru dimnog oblaka zapremine 1 m³, procenjene optimalne mase uzorka su 3,25 g i 2,30 g pri nivoima relativne vlažnosti od 65% i 90%. Takođe, povećanjem sadržaja legure Mg-Al povećava se emisija infracrvenog zračenja u β opsegu (3–5 μm), dok emisija u γ opsegu (8–14 μm) opada.

Zaključak: Karakteristike zaklanjanja lasera dimnih smeša na bazi RP/Mg-Al mogu se efikasno kontrolisati optimizacijom sadržaja RP/Mg-Al i nivoa relativne vlažnosti. Takođe, smeše na bazi RP/Mg-Al pokazuju izražene karakteristike infracrvenog zračenja koje su takođe pod uticajem sadržaja crvenog fosfora i legure Mg-Al. Težište budućih istraživanja bi trebalo biti usmereno na ispitivanje karakteristika zaklanjanja smeša na bazi RP/Mg-Al u bliskom i dalekom infracrvenom opsegu.

Ključne reči: multispektralni dim, performanse zaklanjanja, karakteristike infracrvenog zračenja, crveni fosfor, legura Mg-Al.

Paper received on: 22 April 2025.
Manuscript corrections submitted on: 16 May 2025.
Paper accepted for publishing on: 4 June 2025.